Received: 7 May 2018 | Revised: 30 June 2019 | Accepted: 10 July 2019

DOI: 10.1111/bph.14830

Themed Section: Mitochondrial Pharmacology: Featured Mechanisms and Approaches for Therapy Translation

RESEARCH PAPER

Inhibiting nucleolin reduces inflammation induced by mitochondrial DNA in cardiomyocytes exposed to hypoxia and reoxygenation

Lars Henrik Mariero[1,2] | May-Kristin Torp[1,2] | Christina Mathisen Heiestad[1,2] | Anton Baysa[1,2] | Yuchuan Li[1] | Guro Valen[1,2†] | Jarle Vaage[3,4] | Kåre-Olav Stensløkken[1,2]

[1] Department of Molecular Medicine, Division of Physiology, Institute of Basic Medical Sciences, Faculty of Medicine, University of Oslo, Oslo, Norway

[2] Center for Heart Failure Research, Faculty of Medicine, University of Oslo, Oslo, Norway

[3] Institute of Clinical Medicine, University of Oslo, Oslo, Norway

[4] Department of Emergency Medicine and Intensive Care, Oslo University Hospital, Oslo, Norway

Correspondence
Kåre-Olav Stensløkken, Division of Physiology, Department of Molecular Medicine, Institute of Basic Medical Sciences, Faculty of Medicine, University of Oslo, Domus Medica, Sognsvannsveien 9, Oslo 0372, Norway.
Email: k.o.stenslokken@medisin.uio.no

Funding information
Novo Nordisk, Grant/Award Number: NNF13OC0005157; South-Eastern Norway Regional Health Authorities, Grant/Award Number: 2015095; Novo Nordisk Foundation; Norwegian Health Association; The Norwegian Research Council, Grant/Award Number: 214557

Background and purpose: Cellular debris causes sterile inflammation after myocardial infarction. Mitochondria constitute about 30 percent of the human heart. Mitochondrial DNA (mtDNA) is a damage-associated-molecular-pattern that induce injurious sterile inflammation. Little is known about mtDNA's inflammatory signalling pathways in cardiomyocytes and how mtDNA is internalized to associate with its putative receptor, toll-like receptor 9 (TLR9).

Experimental Approach: We hypothesized that mtDNA can be internalized in cardiomyocytes and induce an inflammatory response. Adult mouse cardiomyocytes were exposed to hypoxia-reoxygenation and extracellular DNA. Microscale thermophoresis was used to demonstrate binding between nucleolin and DNA.

Key results: Expression of the pro-inflammatory cytokines IL-1β and TNFα were upregulated by mtDNA, but not by nuclear DNA (nDNA), in cardiomyocytes exposed to hypoxia-reoxygenation. Blocking the RNA/DNA binding protein nucleolin with midkine reduced expression of IL-1β/TNFα and the nucleolin inhibitor AS1411 reduced interleukin-6 release in adult mouse cardiomyocytes. mtDNA bound 10-fold stronger than nDNA to nucleolin. In HEK293-NF-κB reporter cells, mtDNA induced NF-κB activity in normoxia, while CpG-DNA and hypoxia-reoxygenation, synergistically induced TLR9-dependent NF-κB activity. Protein expression of nucleolin was found in the plasma membrane of cardiomyocytes and inhibition of nucleolin with midkine inhibited cellular uptake of CpG-DNA. Inhibition of endocytosis did not reduce CpG-DNA uptake in cardiomyocytes.

Conclusion and implications: mtDNA, but not nDNA, induce an inflammatory response in mouse cardiomyocytes during hypoxia-reoxygenation. In cardiomyocytes, nucleolin is expressed on the membrane and blocking nucleolin reduce inflammation. Nucleolin might be a therapeutic target to prevent uptake of immunogenic DNA and reduce inflammation.

Abbreviations: DAMP, damage-associated (or danger-associated) molecular pattern; HDAC2, histone deacetylase 2; mtDNA, mitochondrial DNA; Ncl, nucleolin; NCX, sodium–calcium exchanger; nDNA, nuclear DNA; NLR, nucleotide-binding oligomerization domain (NOD)-like receptor; qPCR, quantitative real-time PCR; Rpl 32, 60S ribosomal protein L32; SAP, stable angina pectoris; STEMI, ST elevation myocardial infarction

Lars Henrik Mariero and May-Kristin Torp shared first authorship.

†Professor Valen passed away September 26, 2014.

LINKED ARTICLES: This article is part of a themed section on Mitochondrial Pharmacology: Featured Mechanisms and Approaches for Therapy Translation. To view the other articles in this section visit http://onlinelibrary.wiley.com/doi/10.1111/bph.v176.22/issuetoc

1 | INTRODUCTION

After myocardial infarction, debris from necrotic cardiac cells and extracellular matrix activates the innate immune system (Frangogiannis, 2014). Endogenous molecules that trigger the innate immune system are called damage-associated molecular patterns (DAMPs; Seong & Matzinger, 2004). DAMPs stimulate receptors of the innate immune system including **nod-like receptors (NLRs)** and **toll-like receptors (TLRs**; Arslan, de Kleijn, & Pasterkamp, 2011). DAMPs released from post-ischaemic cardiomyocytes may include high-mobility group box 1 (Andrassy et al., 2008; Ding et al., 2013), heat-shock proteins (Dybdahl et al., 2005; Gupta & Knowlton, 2007; Tian et al., 2013; Zou et al., 2008), ATP (la Sala et al., 2003), uric acid (Shi, Evans, & Rock, 2003), and mitochondrial DNA (mtDNA; Nakayama & Otsu, 2018).

Mitochondria occupy 30% of the volume of the human heart (Barth, Stammler, Speiser, & Schaper, 1992), and we have shown that mtDNA is released into the circulation from the heart of patients with ST elevation myocardial infarction (STEMI) after primary percutaneous coronary intervention (Bliksoen et al., 2012). mtDNA has been suggested to resemble bacterial DNA which contains pro-inflammatory, unmethylated CpG motifs (Collins, Hajizadeh, Holme, Jonsson, & Tarkowski, 2004; Pollack, Kasir, Shemer, Metzger, & Szyf, 1984). mtDNA has been shown to induce sterile inflammation through the intracellular **TLR9** receptor in human neutrophils (Zhang et al., 2010). The mitochondria have a central role in reperfusion injury in general (Kloner et al., 2017). Moreover, in pressure-overloaded mice, DNase activity or ablation of TLR9 disrupts the deleterious inflammatory response to mtDNA and improves survival after transaortic constriction (Oka et al., 2012). mtDNA triggers NF-κB activation possibly by a TLR9-dependent mechanism in an in vivo mouse model and in HEK293 cells (Bliksoen et al., 2016). Still, the mechanism for mtDNA to activate an immune response in primary cardiac cells, and how mtDNA may be internalized, remains unknown.

Many DAMPs are recognized by intracellular receptors (Nunez, 2011), and though ligand–receptor interaction is obligate for host recognition and response, the mechanisms of DAMP internalization are poorly understood. TLR9 is an intracellular receptor located in the endosome (Hemmi et al., 2000) and inhibiting the uptake of DNA ligands of TLR9 is a possible mechanism for modulating TLR9-mediated immune responses. Nucleolin is a multifunctional protein abundant in the nucleolus of eukaryotic cells (Tajrishi, Tuteja, & Tuteja, 2011). It is subject to post-translational modification and regulation and contains four DNA-binding sites as well as numerous glycosylation and phosphorylation sites (Cong, Das, & Bouvet, 2011). Nucleolin is implicated in ribosome maturation, RNA and DNA metabolism, and shuttling of pre-RNAs from the nucleus to the cytoplasm (Medina, Fernando, Isabel Manzano, Manrique, & Herranz, 2010; Tajrishi et al., 2011). The function of nucleolin in the heart is poorly understood. In a study of 71 explanted human hearts, nucleolin mRNA and protein were increased in both ischaemic and dilated cardiomyopathy compared to control hearts, and nucleolin expression correlated with left-ventricular end-diastolic diameter (Rosello-Lleti et al., 2012). Mice overexpressing nucleolin had reduced infarct size in an in vivo model of 30 minutes ischaemia followed by 24hours reperfusion (Jiang et al., 2013). Nucleolin has been implicated in ischaemic preconditioning of the heart (Jiang et al., 2014), and heat-shock proteins may mediate the protective effects of nucleolin (Jiang et al., 2010; Jiang et al., 2013; Jiang et al., 2014). Cell-surface nucleolin has been implicated in internalization of human immunodeficiency virus in T lymphocytes (Said et al., 2002), uptake of DNA nanoparticles (Chen, Kube, Cooper, & Davis, 2008), and as a target for a 26 base pair anticancer DNA aptamer (Soundararajan et al., 2009).

We hypothesized that extracellular DNA, including mtDNA, triggers innate immunity signalling in primary cardiac cells exposed to hypoxia/reoxygenation (H/R) via TLR9 and that nucleolin on the cell surface is responsible for internalizing extracellular DNA in primary cardiac cells.

What is already known

- Extracellular mitochondrial DNA is internalized through an unknown mechanism and cause injury to cardiac cells.

What this study adds

- Extracellular mitochondrial DNA binds to nucleolin.
- Extracellular mitochondrial DNA is internalized by nucleolin, and blocking nucleolin reduces mitochondrial DNA-induced inflammation.

What is the clinical significance

- Nucleolin might be a therapeutic target to reduce uptake of immunogenic DNA, thus decreasing inflammation.

2 | METHODS

2.1 | Experimental animals

All animal care and experimental procedures were approved and conducted in accordance with the Norwegian Animal Health Authority

(FOTS application number 7710). Animal studies are reported in compliance with the ARRIVE guidelines (Kilkenny et al., 2010) and with the recommendations made by the *British Journal of Pharmacology*. C57BL/6 male mice (NOVA-SCB, Nittedal, Norway) weighing 26 ± 0.4 g (age 10–16 weeks, n = 75 for the entire study) with conventional microbiological status were kept in a controlled environment (12:12-hr light/dark period; 23°C; 55–60% humidity; and free access to water and chow [RM3; NOVA-SCB]). Animals were acclimatized for at least 7 days before the experiments. Mice were anaesthetized by intraperitoneal injection of sodium pentobarbital (50 mg·kg^{-1}) and 500 IU heparin (Leo Pharma A/S, Denmark) and killed by cervical dislocation for collection of the liver (to isolate mtDNA) and the heart for subsequent perfusion.

2.2 | Isolation of cardiomyocytes and cardiac fibroblasts

Adult murine cardiomyocytes were isolated with a modified method originally described by O'Connell, Rodrigo, and Simpson (2007). In short, hearts were cannulated and retrogradely perfused at 4 ml·min^{-1} with perfusion buffer (containing in mM: NaCl 120.4; KCl 14.7; KH_2PO_4 0.6, Na_2HPO_4 0.6; $MgSO_4$ 1.2; Na-HEPES 10.0; glucose 5.5; $NaHCO_3$ 4.6; taurine 30.0; BDM 10.0) before switching to collagenase II digestion (#4177, batch 44C14813, activity 385 U·mg^{-1}, Worthington, Lakewood, NJ, USA), low-speed centrifugation (20 × g), and gradual calcium reintroduction. Isolated cardiomyocytes were resuspended in plating medium containing MEM (minimal essential medium) with Hanks BSS (balanced salt solution; #M5775), 10% FBS (#SH30073.03, lot #AVA60491, Thermo Fisher Scientific, MA, USA), 10-mM BDM (2,3-butanedione monoxime, #B0753), 100 U·ml^{-1} penicillin–streptomycin (#P4333), and 2-mM L-glutamine (#G7513) and left to attach on laminin-coated plates (1 µg·cm^{-2}, # 354232, BD Biosciences, East Rutherford, NJ, USA) for 1–2 hr at 37°C and 2% CO_2. After plating medium was removed, short-term culture medium was added (MEM with the same antibiotic and L-glutamine supplements as plating medium, but with 0.10% fatty-acid free BSA [#A8806] instead of FBS and 1-mM BDM).

Cardiac fibroblasts were isolated from the supernatant of the first low-speed centrifugation by re-centrifuging twice for 5 min at 700× g. The cells were resuspended in fibroblast medium containing MEM with Hanks BSS, 10% FBS (#10270-106, lot #41Q3723K, Life Technologies), and 100 U·ml^{-1} penicillin–streptomycin and 2-mM L-glutamin and seeded in uncoated flasks. The cardiac fibroblasts were kept at 37°C and 5% CO_2 and passaged three times (1–2 weeks) before they were used in experiments and are referred to as cultured cardiac fibroblasts (C-CF). For some applications, freshly isolated cardiac fibroblasts were used, referred to as CF. The purity of the cell fractions was evaluated by qPCR (Figure S1). PCR primer sequences are listed in Table S1. Cells were confirmed mycoplasma-free.

For the cytokine expression in cardiomyocytes, two series of experiments were performed at two different times. In the first series (Figure 1a–c, n = 6), primary cardiomyocytes were seeded into six parallels, while in the second series (Figure 1d–f, n = 12), five parallels were used.

2.3 | Isolation of mitochondrial and nuclear DNA

C57BL/6 mice were killed by cervical dislocation, and livers were quickly extracted and washed in ice-cold sterile PBS. Mitochondria were isolated using a 2-mL Kontes Dounce tissue grinder and the Mitochondria Isolation Kit for Tissue (#89801, Thermo Fisher Scientific, Waltham, MA, USA) according to the manufacturer's instructions, by initial centrifugation at 700× g and 3,000× g and with two additional washing steps with buffer C. The pellet after the first centrifugation at 700× g was used to isolate nuclear DNA (nDNA). DNA was isolated using spin columns (#69506, Qiagen DNeasy Blood & Tissue, Venlo, Netherlands) according to the manufacturer's instructions. mtDNA was extracted from isolated mitochondria and nDNA from crude nuclear extracts, both from mouse liver tissue. DNA was fragmented on ice using a 30-kHz/50-W ultrasonic sonicator (#UPH50, Hielscher Ultrasonics, Teltow, Germany) with a 0.5-mm head at 14 µm for 2 × 30 s. Fragmentation after ultrasonification was visualized on a 1% agarose gel with SYBR safe DNA dye (#33012, Life Technologies, Carlsbad, CA, USA), and the relative abundance of mtDNA and nDNA was determined by qPCR (Figure S2). Calculations and estimation of the absolute concentrations of mtDNA and nDNA in the two fractions are described in detail in the Supporting Information. In brief, calculations from the qPCR reaction indicate that the mitochondrial fraction contains at least 5 µg·ml^{-1} mtDNA and 15 µg·ml^{-1} nDNA while the nuclear fraction only contains nDNA. Inspection of the agarose gels (Figure S2) indicated breaks in the non-sonicated mtDNA, which could underestimate the actual amount of mtDNA measured by qPCR. As nDNA contained no mtDNA, the differences found in the response are likely to be due to the presence or not of mtDNA. In the discussion, we therefore refer to mtDNA and nDNA, while in the figures, we describe the doses as mtDNA-enriched extracellular DNA and nDNA.

2.4 | Hypoxia/reoxygenation (H/R) model

The oxygen concentration in culture medium was measured with a galvanometric oxygen electrode, (Oxi 323, WTW, Weilheim, Germany, Figure S3A). Glucose-free DMEM (#D5030-1L) was left in <0.5% O_2, 2.0% CO_2 overnight in a hypoxia chamber (#856-HYPO, Plas Labs, Lansing, MI, USA) prior to experiments. Cells were brought into the chamber, washed once with hypoxic medium (to wash out oxygen on tissue culture plate and medium, Figure S3B), and exposed to hypoxic conditions for 40 min before reoxygenation in normal glucose-containing medium in a normoxic incubator. Control cells followed the same protocol as cells exposed to H/R, but without hypoxia. Cell death was assessed by LDH release (Cytotoxicity Detection Kit, Roche, Penzberg, Germany). The nucleolin inhibitor midkine (#SRP3301) was dissolved in PBS and 0.1% BSA to a stock solution (74.6 µM) and dissolved to a final concentration of

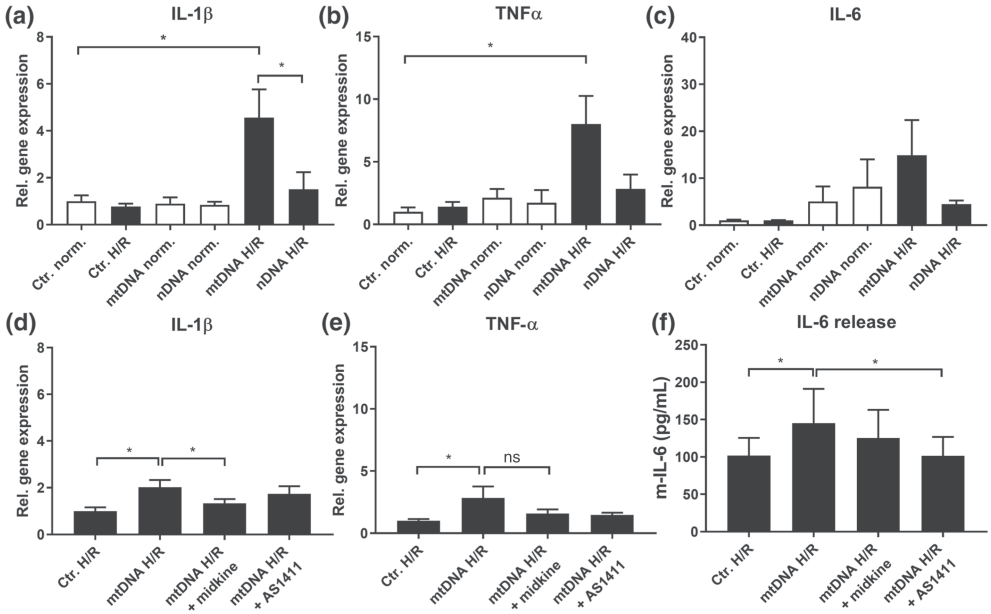

FIGURE 1 mtDNA-induced inflammation in cardiomyocytes during hypoxia/reoxygenation (H/R) is reduced by blocking nucleolin. Quantitative real-time PCR on isolated adult C57BL/6 murine cardiomyocytes exposed to 40 min of non-lethal glucose-free hypoxia (<0.5% O_2) followed by 2 hr of reoxygenation (Ctr. H/R) or time-matched normoxic conditions with medium change (Ctr Norm.) was performed. Cells were exposed to murine mitochondrial DNA-enriched fraction (20 μg·ml^{-1} total, >5-μg mtDNA, <15 μg·ml^{-1} nDNA) or nuclear DNA (nDNA, 20 μg·ml^{-1}, nDNA H/R) in normal medium (mtDNA norm and nDNA norm) or in combination with H/R (mtDNA H/R and nDNA H/R). Two independent series of experiments were conducted; (a–c) n = 6 and (d–f) n = 12. The data shows relative gene ($2^{-\Delta\Delta Ct}$) expression of (a) IL-1β, (b) IL-6, or (c) TNF-α. (d) and (e) shows expression of IL-1β and TNF-α exposed to mtDNA-H/R and blockade of nucleolin with either midkine (200 nM) or the aptamer AS1411 (10 μg·ml^{-1}). Data are relative to the expression of the housekeeping gene Rpl32 and normalized to (a–c) normoxic control cells or (d–f) hypoxic cells. (f) ELISA of media at the end of the reoxygenation protocol shows release of IL-6 from mouse cardiomyocytes. Data are presented as mean ± *SEM*. In a-c, **P* < .05, significantly different as indicated; Kruskal–Wallis test with a Dunn post-test. In d-f, **P* < .05, significantly different as indicated; Freidman ANOVA with Dunn post-test

200 nM. The aptamer AS1411 (Invitrogen, sequence in Table S2) was dissolved in endotoxin-free water and refolded according to the manufactures protocol at 65°C for 15 min (stock 1 mg·ml^{-1}). Fresh aliquots were prepared at the day of the experiments. For each media change, new mtDNA and blockers were added to the respective groups. The vehicle control groups received similar media change. As there are some day-to-day variability in the response from isolated cardiomyocytes and the HEK293 cells, the data are normalized to the control groups.

2.5 | Assessing TLR9-dependent NF-κB activity and cytokine expression in HEK293 cells

TLR9-dependent NF-κB activity was assessed using commercially available HEK293 cells co-transfected with mouse TLR9 and an inducible secreted embryonic alkaline phosphatase (SEAP) reporter coupled to NF-κB (HEK-Blue mTLR9, RRID:CVCL_IM93, Invivogen, Toulouse, France). Cells without TLR9 (HEK-Blue Null1) served as controls, and all cells were cultured according to instructions of the manufacturer. NF-κB reporter activity was quantified with spectrophotometer. In H/R experiments, the hypoxia protocol was as previously described with reoxygenation for 6–12 hr. The cells were exposed to treatments, including CpG A (20 μg·ml^{-1}, ODN2216, Invivogen), CpG B (20 μg·ml^{-1}, ODN1668, Invivogen), inhibitory CpG (CpGi, 20 μg·ml^{-1}, ODN2088), chloroquine (#C6628, 100 ng·ml^{-1}), or the nucleolin inhibitor midkine.

To investigate endogenous cytokine expression, HEK293-Blue Null1 cells were plated at a density of 70,000 HEK293 cells in each well in a 12-well plate and left overnight. Cells were exposed to 20 μg·ml^{-1} mtDNA or 20 μg·ml^{-1} nDNA overnight (approximately 20 hr). Cells were washes twice with 1X PBS before lysed in RLT buffer. AE buffer was used as vehicle control. RNA, cDNA, and qPCR were done in same way as previous with cardiomyocytes (primer sequences in Table S3).

2.6 | Transfection of HEK293 cells

Transfection with Lipofectamine® 2000 Transfection Reagent (#11668027, Thermo Fisher Scientific, Massachusetts, USA) was performed according to manufacturers' protocol. In short, cells were seeded at a density of 2.8 × 10^4 cells·cm^{-2} 1 day prior to transfection. At the day of transfection, cells were washed twice and kept in antibiotic-free medium. DNA (0.5 μg·cm^{-2}; GFP-nucleolin plasmid [#28176, Addgene, Massachusetts, USA]) and lipofectamine were diluted in Opti-MEM (#31985070, Thermo Fisher Scientific, Massachusetts, USA) before the two solutions were combined and added to the cells. After 4-hr incubation (37°C, 5% CO_2), DNA-lipofectamine complexes were exchanged for normal cell medium; 48 hr post

transfection, efficiency was evaluated visually, based on GFP-positive cells, with a Nikon Eclipse TS100 microscope (Nikon, Tokyo, Japan) with an Omron H7ET Nikon illumination system (Nikon, Tokyo, Japan), and pictures taken with Digital Sight DS-LE (Nikon, Tokyo, Japan). Overexpression of nucleolin was investigated with western blotting and with confocal microscopy.

2.7 | Protein expression of recombinant nucleolin and MST binding assay

2.7.1 | Protein expression and purification

A pET28b plasmid containing a codon optimized nucleotide sequence of human nucleolin (residues 300–650, inserted between the NdeI and BamHI restriction sites) was transformed into *Escherichia coli* BL21-CodonPlus (DE3)-RIPL competent cells by heat pulse (Agilent). The transformed cells were grown to an OD_{600} of 0.5 at 37°C in 2 L of LB medium supplemented with kanamycin before the temperature was lowered to 18°C, and the culture was induced with 0.25-mM isopropyl β-D-thiogalactoside and left overnight for expression of the N-terminal His-tagged nucleolin. The cell culture was centrifuged at 6,500× *g* for 20 min, and the cell pellet was dissolved in 60 ml of sonication buffer (300-mM NaCl, 10-mM imidazole, 10-mM TRIS pH 8, 10-mM β-mercaptoethanol; buffer 1). Cells were lysed by 3 × 30 s sonication, and a cell-free extract was prepared by centrifugation at 27,000× *g* for 20 min. The protein was purified using cobalt and nickel ion-metal affinity chromatography (IMAC) with Ni-NTA agarose and buffer 1 supplemented with 50-mM imidazole. Fractions rich in nucleolin were pooled and dialysed against PBS.

2.7.2 | Microscale thermophoresis (MST)

MST was used to study the interaction of nucleolin with mitochondrial (mt) and nuclear (n) DNA. The purified nucleolin was labelled with the NT-647 RED-tris-NTA dye for His-tagged proteins following the recommended labelling protocol (Nanotemper Technologies). In brief, 100 µl of 200-nM protein was mixed with 100 µl of 100-nM dye and incubated at room temperature for 30 min. The labelled protein was added to a 1:1 dilution series of the DNA in buffer X to a final concentration of 50 nM. The mtDNA concentration was diluted 16 times relative to the nDNA (in $mg{\cdot}ml^{-1}$). The 16 different samples were left for a few minutes before loaded into premium coated NT.115 MST capillaries (Nanotemper). Fluorescence profiles were measured at 25°C in a Monolith NT.115 instrument using the red channel. Data were collected at 60% MST power and 80% excitation power, and the fluorescence signals during the thermophoresis were monitored for 30 s. The changes in fluorescence (ΔF_{norm}) due to thermophoresis were measured as the signal difference between time points 0 and 5 s. Data were normalized and plotted as a function of the ligand concentration, and a binding curve was fitted to the average of three independent dilution series of each form of the DNA. The concentration of the DNA was calculated using an average molecular mass of DNA corresponding to 300 base pairs, as taken from the agarose gel analysis of the sonicated DNA (Figure S2C).

2.8 | Quantification of CpG and dextran uptake in cardiac cells

Primary cardiomyocytes or cultured cardiac fibroblasts were seeded on eight-well chamber slides (#154534, LabTek, Thermo Scientific) and incubated with 20 $\mu g{\cdot}ml^{-1}$ FITC-labelled CpG C (ODN2395f, Invivogen) for ~16 hr before staining with 0.7 $\mu g{\cdot}ml^{-1}$ Hoechst 33342 (Life Technologies) and mounting (gelatin [166 $mg{\cdot}ml^{-1}$] in water and 50% glycerol). Automated image acquisition and analysis was performed using an Olympus Scan^R fluorescent microscope. In brief, the microscope acquires a predefined number of images at the same place in each well (25 images per well in this experiment), assuring objectivity for the acquisition. The software allows detailed resolution and objectivity as the software only allows equal thresholds for all scanned images. For cardiomyocytes, the average maximum fluorescence was used as a measure for CpG and dextran (D22910, 10,000 MW, molecular probes, Invitrogen) uptake. For evaluation of endocytosis, the cardiomyocytes were incubated overnight with dextran with or without cytochalasin D (10 or 50 µM) or dynasore (10 or 25 µM). For cardiac fibroblasts, CpG was analysed, and the average fluorescence per spot was used. The analysis settings were different because the number of spots was lower in the cardiomyocytes and not all cells contained fluorescent signal. Though the uptake of CpG by different cell types could not be appropriately analysed by the same parameters, equal automated settings were applied within each cell type. Cardiomyocytes or cardiac fibroblasts were treated without CpG, with CpG or with CpG and 200-nM midkine or midkine alone. To confirm that the signals were intracellular, confocal microscopy was performed using a Zeiss LSM700 or 710.

2.9 | Gene expression analysis

At the end of experiments, cells were washed once with PBS, lysed with 350-µl RLT buffer supplemented with 1% β-mercaptoethanol, and snap-frozen in liquid nitrogen. Cells were mechanically disrupted in a beadmill (FastPrep FP120, MP Biomedicals, Santa Ana, CA, USA), and RNA was extracted using RNeasy columns and treated with RNAse-free DNAse (both Qiagen). cDNA was reverse transcribed from 100-ng RNA in 20 µl using qScript cDNA SuperMix (#95048, Quanta Biosciences, Gaithersburg, MD, USA) according to instructions of the manufacturer. Minus reverse transcriptase control was included. qPCR was performed using SYBR Green (#4368706, Life Technologies) for nucleolin (Ncl), **IL-1β**, **IL-6**, **TNF-α**, and Rpl32 as endogenous control on a 7900HT qPCR machine (Applied Biosystems). Primer efficiency was measured for each qPCR reaction using a standard curve on each individual plate. All reactions were normalized according to $\Delta\Delta C_q$ method to a reference gene (Rpl32 for cardiomyocytes and GAPDH for HEK293 cells).

2.10 | Subcellular protein fractionation

Subcellular protein fractionation was performed using the Compartment Protein Extraction Kit (#2145, Merck Millipore, Billerica, MA, USA) according to instructions of the manufacturer with an additional 700× *g* centrifugation step after cell lysis to reduce nuclear carry-over to the membrane fraction.

2.11 | Immunoblotting

The immuno-related procedures used comply with the recommendations made by the *British Journal of Pharmacology*. Protein expression of nucleolin in cardiomyocytes and cardiac fibroblasts and in different cardiomyocyte compartments as well as the purity of subcellular fractions were investigated by immunoblotting. In brief, 2.5-μg protein per lane was separated on gradient SDS gels, transferred to nitrocellulose membranes, and imaged with autoradiography using X-ray film with enhanced chemiluminescence. Reversible Ponceau staining was used as a loading control. For additional information, see Supporting Information.

2.12 | ELISA

ELISA kits were purchased from R&D systems (R&D Systems, Inc., Minneapolis, USA), and the protocol was conducted according to the manufacturer. In brief, capture antibodies were diluted in PBS and added to high-binding 96-well plates 1 day in advance of the experiment. Plates were blocked with reagent diluent (1% BSA in PBS) and washed with washing buffer (0.05% Tween 20 in PBS). Substrate solution was purchased from Life Technologies (TMB Single solution, Thermo Fisher Scientific Inc.), and H_2SO_4 was used as stop solution. Absorbance was measured at 450 and 570 nm with BioTek PowerWave XS (BioTek, Vermont, USA).

2.13 | Data and statistical analysis

The data and statistical analysis comply with the recommendations of the *British Journal of Pharmacology* on experimental design and analysis in pharmacology. Unless otherwise stated, data are presented as mean ± *SEM*. For paired multigroup comparisons, a Freidman ANOVA with Dunn post-test was used. For non-paired analysis, a Kruskal–Wallis with a Dunn post-test was used. For NF-κB activity in mtDNA/nDNA-treated reporter cells, a Student's *t* test was used. Graphpad (RRID: SCR_000306) 6.05 was used for all statistical analyses (La Jolla, CA, USA), and $P < 0.05$ was considered statistically significant.

2.14 | Materials

Unless otherwise stated, all compounds and reagents were purchased from Sigma-Aldrich (St. Louis, MO, USA).

2.15 | Nomenclature of targets and ligands

Key protein targets and ligands in this article are hyperlinked to corresponding entries in http://www.guidetopharmacology.org, the common portal for data from the IUPHAR/BPS Guide to PHARMACOLOGY (Harding et al., 2018), and are permanently archived in the Concise Guide to PHARMACOLOGY 2017/18 (Alexander, Fabbro et al., 2017a, b; Alexander, Kelly, et al., 2017).

3 | RESULTS

3.1 | Blocking nucleolin reduce mtDNA-induced inflammation after hypoxia/reoxygenation in cardiomyocytes

In cardiomyocytes exposed to normoxic conditions, neither mtDNA nor nDNA induced pro-inflammatory genes downstream of NF-κB (Figure 1 a–c). When cardiomyocytes were exposed to non-lethal H/R, mtDNA-induced expression of IL-1β and TNF-α, but this effect was reduced when nucleolin was inhibited (Figure 1d,e). nDNA did not induce any IL-1β and TNF-α after H/R (Figure 1a–c). The aptamer AS1411 also significantly reduced IL-6 release from cardiomyocytes exposed to H/R (Figure 1f). Neither midkine nor AS1411 alone affected IL-1β and TNF-α expression in adult mice cardiomyocytes (Figure S4E,F). The present model of H/R did not induce cell death (Figure S4A,B), but longer duration of hypoxia yielded cell death (Figure S4C). H/R alone did not increase expression of inflammatory genes in cardiomyocytes (Figure S4D). In control experiments, glucose-free DMEM was supplemented with glucose, and there was no effect on viability of cardiomyocytes as compared to standard medium.

3.2 | Hypoxia/reoxygenation induces TLR9-dependent NF-κB activity in HEK293 reporter cells

In HEK293 reporter cells, H/R-induced NF-κB activity after ~6–7 hr of reoxygenation (Figure S5A,B,D,E), and NF-κB activity was increased at 8 hr (Figure 2a). In normoxia, both CpG A and CpG B induced NF-κB activity over time-matched control (Figure 2a). In normoxia, CpG B induced NF-κB activity more than three times higher than CpG A (Figure 2a).

CpG A and CpG B stimulation acted in concert with H/R to more than double the NF-κB activity compared to H/R alone (Figure 2a). TLR9 dependence was confirmed with the use of a TLR9 null cell line with the same NF-κB reporter system (Figure S5A–C). In hypoxia, the effect of CpG B was inhibited by CpGi or chloroquine (Figure 2b). Furthermore, CpGi or chloroquine also inhibited the synergistic effect of CpG A and H/R (Figure 2c). The temporal effects of CpG A inhibition in H/R by CpGi and chloroquine are shown in Figure S5F,G.

mtDNA, but not nDNA, stimulated NF-κB activity in normoxic HEK293 cells overexpressing TLR9, but there was no synergistic effect on NF-κB activity between DNA ligands and H/R (Figure 2d). In HEK293 null cells, mtDNA but not nDNA increased expression of IL-6 (Figure S6A). Extracellular DNA did not increase expression of TNFα in HEK293 cells (Figure S6B).

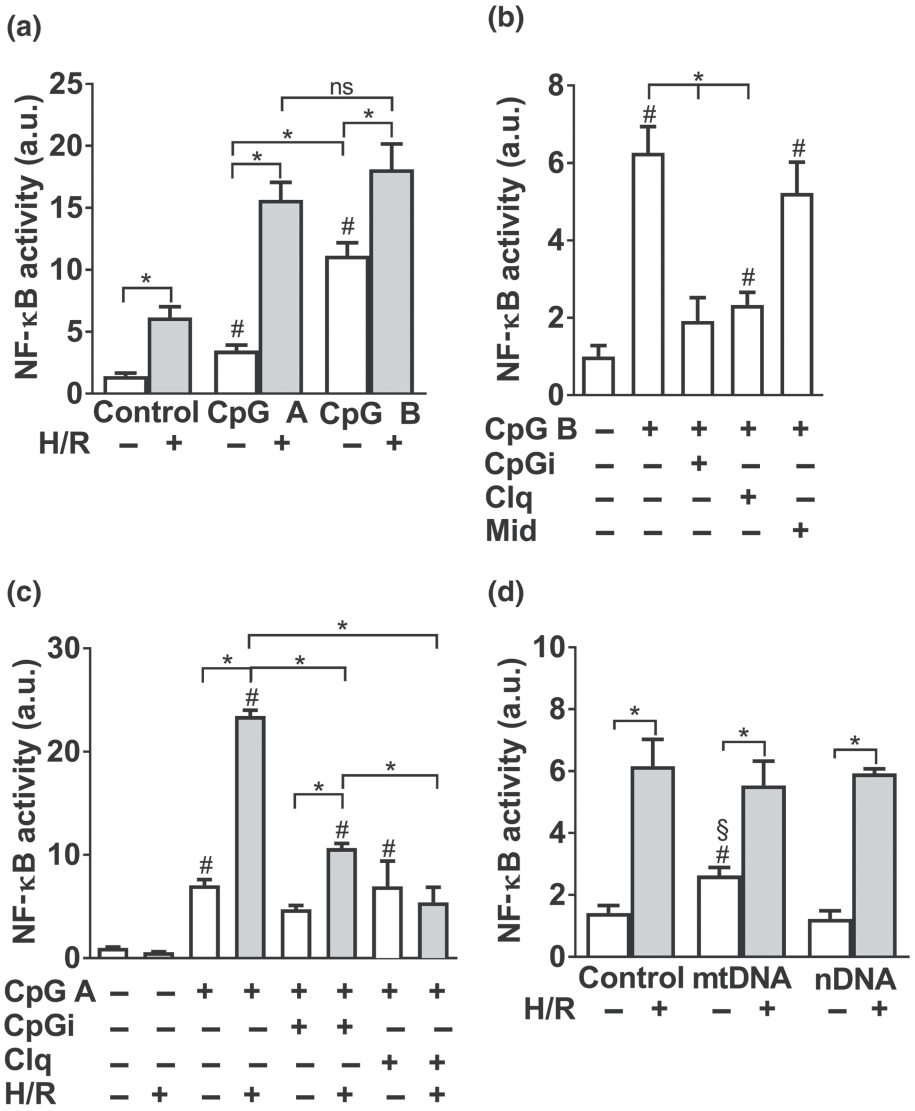

FIGURE 2 Extracellular DNA induces NF-κB activity in HEK293 cells. (a) HEK293 NF-κB reporter cells overexpressing murine TLR9 were exposed to 40 min of hypoxia with 8-hr reoxygenation (H/R) in combination with either control, 20 μg·ml^{-1} CpG A or CpG B. (b) NF-κB activity in HEK293 cells exposed to CpG B and inhibitory CpG (CpGi, ODN 2088, 20 μg·ml^{-1}), chloroquine (Clq, 100 ng·ml^{-1}) or midkine (Mid, 200 nM) during 40 min of hypoxia and 6 hr of reoxygenation. (c) HEK293 cells exposed to 40 min of hypoxia and reoxygenation for 12 hr (H/R) and combinations of CpG A and CpGi or chloroquine. (d) NF-κB activity after 40 min of hypoxia and 6 hr of reoxygenation (H/R) and 20 μg·ml^{-1} mitochondrial DNA (mtDNA enriched <5-μg mtDNA, >15 μg·ml^{-1} nDNA mtDNA) or nuclear DNA (nDNA). The data shown are means ± *SEM* (n = 5). *P < .05, significantly different as indicated; #P < .05; significantly different from control, §P < .05, significantly different from nDNA. In a-c, one-way ANOVA with Tukey post test wa used; in d, Student's t test was used

Attempts to overexpress nucleolin in HEK293 cells overexpressing TLR9 were not successful as these cells did not survive the procedure, although the TLR9 null cells survived and displayed high expression of nucleolin (Figure 3b).

3.3 | CpG uptake is not mediated by endocytosis in cardiomyocytes

We hypothesized that a DNA uptake mechanism would be sequence and structure independent and investigated the possible role of endocytosis. Using fluorescence-labelled dextran, we established a model of inhibiting endocytosis by cytochalasin D or dynasore in primary mouse cardiomyocytes (Figure S7A,B). There was no effect on the uptake of fluorescent CpG in cardiomyocytes treated with 10- or 50-μM cytochalasin D (Figure, S7D).

3.4 | Nucleolin is expressed in cardiomyocyte membranes

Nucleolin mRNA is abundant in the mouse heart, with lower Ct values in hearts and cardiomyocytes compared to cardiac fibroblasts (Figure S8A). The relative expression of nucleolin in cardiomyocytes is higher than whole heart, freshly isolated cardiac fibroblasts, and cultured cardiac fibroblasts (Figure 3a).

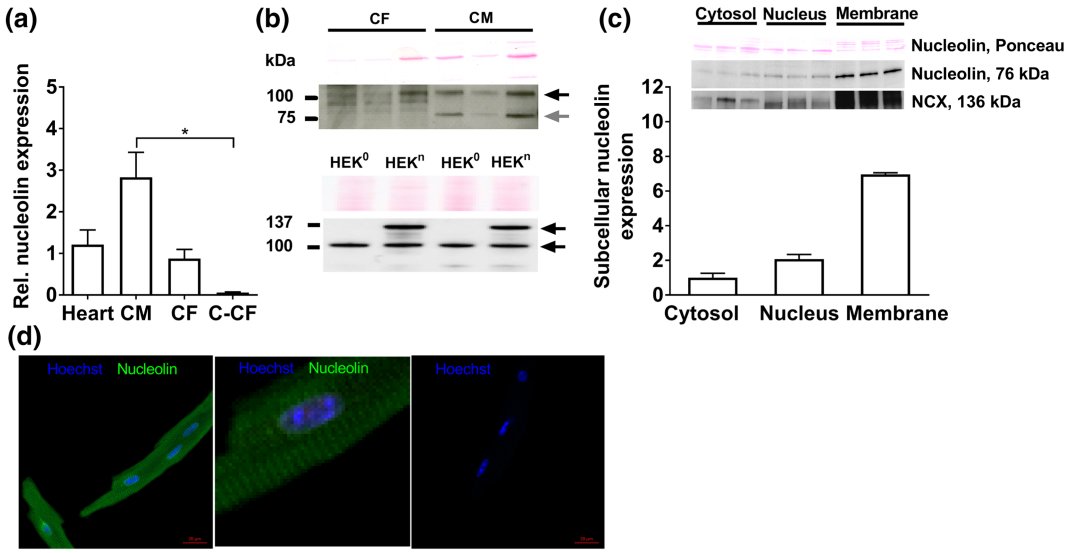

FIGURE 3 Nucleolin is expressed in cardiomyocyte membranes. mRNA isolated from six C57BL/6 mice, whole hearts (Heart), cardiomyocytes (CM), freshly isolated cardiac fibroblasts (CF), and cultured cardiac fibroblasts after three passages (C-CF). (a) Relative quantification of nucleolin normalized to Rpl32 and calibrated to whole heart (n = 6). (b) Immunoblotting against nucleolin in cardiomyocytes and cardiac fibroblasts showed bands at 110 kDa (top black arrow) and a smaller band at 76 kDa (grey arrow). Transfecting HEK293 cells with nucleolin displayed a band at 136 kDa (HEK^n 110 kDa nucleolin +26.9 kDa GFP tag, black arrow) in addition to the constituent HEK293 nucleolin (HEK^0; 110 kDa, black arrow). On top of each blot is the corresponding area with Ponceau staining as loading control. (c) The 76-kDa band in subcellular protein fractions from cardiac myocytes and presence of the membrane marker NCX (136 kDa). Data from the different fractions are found in Figure S8. (d) Representative confocal micrographs of nucleolin immunocytochemistry using non-permeabilized, fixed cardiomyocytes. A striated staining pattern was seen (panel (d), left, magnification in middle) while the signal was absent in cells only stained with secondary antibody and Hoechst (panel (d), right). Data represents mean ± *SEM*. $^*P < .05$, significantly different as indicated; one-way ANOVA and Tukey multiple comparisons test

The expression of nucleolin protein was determined in isolated cardiac myocytes and fibroblasts by immunoblot (Figure 3b). In cardiomyocytes, two clear bands were detected at 75–80 kDa and ~110 kDa, whereas three bands between ~90 and ~110 kDa were detected in cardiac fibroblasts. By subcellular protein fractionation, the predicted ~76-kDa band detected by immunoblotting against nucleolin was abundant in the membrane of cardiomyocytes, (Figure 3c) against both nuclear and cytosolic protein fractions. Immunocytochemistry showed striated nucleolin staining in non-permeabilized cardiomyocytes (Figure 3d). Overexpression of nucleolin in HEK293 cells confirmed the specificity of the antibody (Figure 3b). Confocal image of HEK293 cells indicates that the main site for the overexpression was in the nucleolus in these cells (Figure S8D,E). However, nucleolin also appear in the membrane fractions of HEK293 cells as shown by western blot (Figure S5I).

Expression of the ~100-kDa nucleolin band was the same in nuclear, cytosolic, and membrane fractions (Figure S8B). The purity of the subcellular fractions (Figure S9) was confirmed by immunoblotting against the **sodium–calcium exchanger (NCX1**; membrane), GAPDH (cytosol), and **histone deacetylase 2 (HDAC2**; nucleus).

3.5 | Mitochondrial DNA binds 10-fold more strongly to nucleolin than nuclear DNA

Microscale themophoresis (MST) profiles for nucleolin mixed with mtDNA or nDNA were collected using an NT.115 MST instrument (Figure 4). The ΔF_{norm} signal was calculated for 5 s of thermophoresis, and a binding curve was fitted to each profile. The signal from the labelled protein at 50 nM is at the lower end of the sensitivity of the NT.115 instrument, but at the same, the protein concentration is too high compared with the apparent K_D values to perform a valid curve fitting and calculation of K_D. As the interaction between nucleolin and DNA is so strong, no exact (K_D) could be calculated from the fitted binding curve. However, a range of 1–10 nM and 10–100 nM can be inferred from the binding curves for mtDNA and nDNA, respectively.

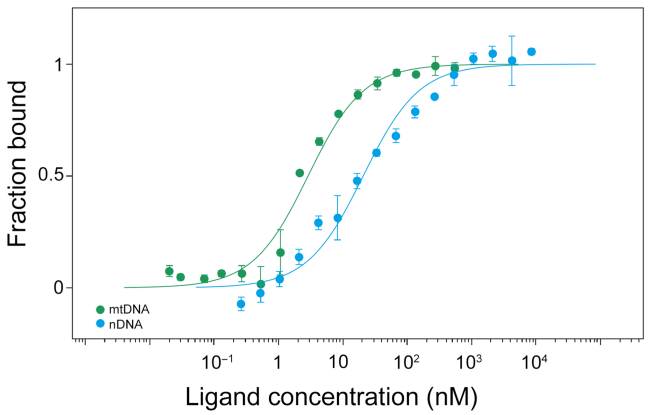

FIGURE 4 Microscale thermophoresis binding curves for nucleolin binding to mtDNA (green) and nDNA (blue). The binding is shown as fluorescence response normalized to binding fraction as a function of DNA concentration and with binding curves for mtDNA and nDNA. The concentration of the DNA is calculated using a molecular mass of DNA fragments corresponding to 300 base pairs

This MST experiment shows that nucleolin interacts directly with mtDNA and that it binds to mtDNA about one order of magnitude more strongly than to nDNA.

3.6 | Nucleolin inhibition reduced uptake of CpG DNA in cardiomyocytes and fibroblasts

As nucleolin is expressed in the membranes of cardiomyocytes, we investigated the effect of nucleolin inhibition on the uptake of fluorescent CpG in cardiac cells. Although not quantified, the uptake of fluorescent CpG appeared higher in cardiac fibroblasts than cardiac myocytes. In isolated cardiomyocytes, the uptake of fluorescent CpG DNA was reduced when the cells were incubated in the presence of the nucleolin inhibitor midkine (Figure 5), and CpG was detected intracellularly in cardiomyocytes by confocal microscopy. Midkine also inhibited the uptake of fluorescent CpG in cardiac fibroblasts (Figure 5). Representative laser scanning confocal micrographs showed attenuation of the intracellular punctuate pattern of fluorescent CpG uptake by midkine treatment. Midkine did not influence cardiomyocyte viability or morphology (Figure S10).

4 | DISCUSSION

We show for the first time that mtDNA rapidly induced an innate immune response in cardiomyocytes exposed to non-lethal H/R and that mtDNA and H/R act in concert to induce NF-κB activity via a TLR9-dependent mechanism. We showed that nucleolin binds more strongly to mtDNA than to nDNA, although it binds both with high affinity. Nucleolin is highly expressed in the heart and is found in the cell membrane of cardiomyocytes. Blocking nucleolin reduced expression of IL-1β and TNF-α and release of IL-6 from cardiomyocytes. The present investigation provides the first evidence of mtDNA and nucleolin binding and that nucleolin may facilitate uptake of immunogenic DNA in primary cultures of cardiac cells.

mtDNA has been shown to be a DAMP in patients with rheumatoid arthritis (Hajizadeh, DeGroot, TeKoppele, Tarkowski, & Collins, 2003) and trauma (Zhang et al., 2010). We have shown that mtDNA is released into the circulation after reperfusion in patients with STEMI (Bliksoen et al., 2012). Our recent findings showed that mtDNA was internalized, activated an NF-κB response, and reduced viability of mouse cardiomyocytes after exposure to mtDNA (Bliksoen et al., 2016). To create a physiologically relevant in vitro model of the metabolic stress of the post-ischaemic extracellular milieu, cardiomyocytes were exposed to mtDNA and H/R. Indeed, these stressors appeared to act in concert to induce pro-inflammatory genes without involvement of specialized immune cells. There was no such effect from nDNA, suggesting that structural or sequence specific properties of the different DNAs guide immunogenicity. It has been suggested that mtDNA resembles bacterial DNA, which contains pro-inflammatory

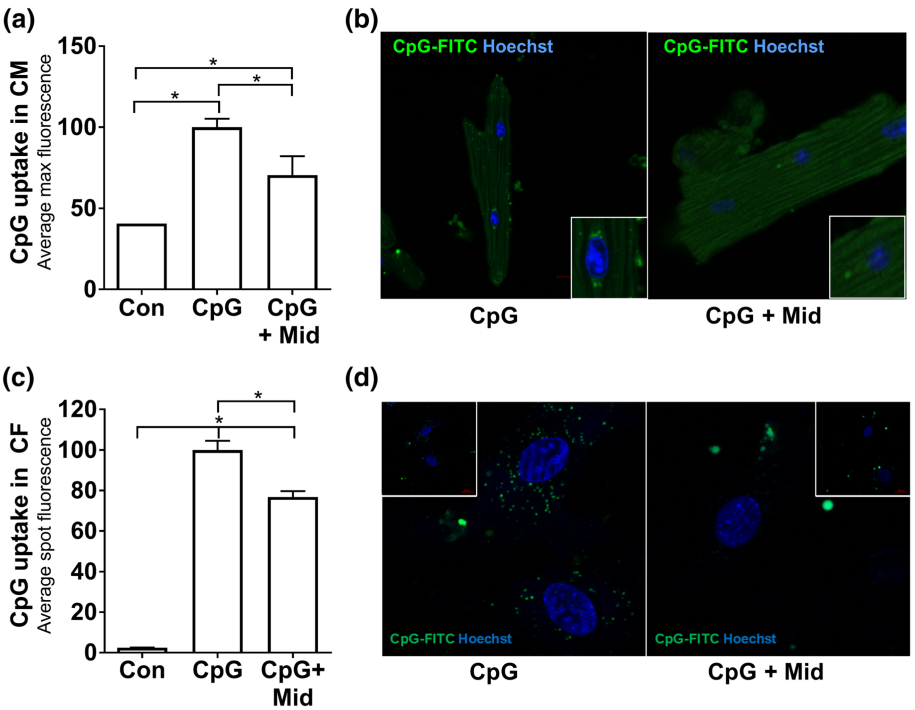

FIGURE 5 Nucleolin inhibition reduces uptake of CpG DNA in cardiac cells. Cardiomyocytes were incubated overnight with no treatment (Con), 20 μg·ml^{-1} fluorescent CpG (CpG), or fluorescent CpG and 200-nM midkine (CpG + Mid). (a) Uptake of fluorescent CpG was evaluated by automated fluorescent microscopy (averaging 3,400 cells from each animal, n = 5, mean ± *SEM*, normalized to CpG group). (b) The uptake of fluorescent CpG in cardiomyocytes was also evaluated by confocal microscopy. The same experiments were performed for cardiac fibroblasts, and the uptake of CpG was quantified using the same method and normalized to CpG: (c) automated fluorescence microscopy and (d) confocal microscopy. *P < .05, significantly different as indicated; one-way ANOVA with Tukey multiple comparisons test

unmethylated CpG motifs (Collins et al., 2004; Pollack et al., 1984) capable of inducing sterile inflammation (Oka et al., 2012; Zhang et al., 2010). In the acute setting of H/R or mtDNA alone, we saw no inflammatory response. H/R and mtDNA appear to signal through both the NF-κB and IFN regulatory factor pathways (Kawai & Akira, 2009), with stronger activation of the former. Moreover, extracellular stressors can also activate the **NLRP3**-inflammasome leading to increased expression of IL-1β (Weber, Wasiliew, & Kracht, 2010). The reduced expression of IL-1β and TNF-α and reduced IL-6 release after nucleolin inhibition indicate that the immune response from mtDNA in cardiomyocytes was blocked at an early stage in the inflammatory pathway. To further investigate the different cellular responses to the mtDNA or nDNA in the H/R-TLR9 setting, we used a reporter system to study the role of TLR9 in synergistic NF-κB activation by H/R and extracellular DNA.

In HEK293 cells, mtDNA but not nDNA induced a NF-κB response. In addition, H/R was a strong inducer of NF-κB activity. Hypoxia has been shown to induce NF-κB activity in the heart (Fitzpatrick et al., 2011), but to our knowledge, this is the first demonstration of synergistic NF-κB activation with concurrent exposure to H/R and extracellular DNA. CpG B is thought to be a more potent inducer of NF-κB signalling than CpG A, whose canonical role is stimulation of the IFN regulatory factor pathway culminating in the release of type 1 IFN (Verthelyi, Ishii, Gursel, Takeshita, & Klinman, 2001). CpG C is a stimulator of both pathways. CpG A induced TLR9-dependent NF-κB activity as potently as CpG B during H/R. The synergistic effect of DNA ligands and H/R should be also considered in other assays when studying inflammatory responses in cardiomyocytes.

Endocytosis did not appear to be involved in internalization of extracellular DNA in cardiomyocytes. Neither cytochalasin D, which depolymerizes filamentous actin to inhibit micropinocytosis (Dutta & Donaldson, 2012), nor the dynamin GTPase blocker dynasore, which inhibits clathrin-mediated endocytosis (Dutta & Donaldson, 2012), inhibited the uptake of CpG into cardiomyocytes. The efficacy of both inhibitors was validated as they inhibited the uptake of fluorescently labelled dextran in cardiomyocytes. These observations suggested a nucleic acid-specific uptake mechanism. Nucleolin is abundant in the heart and shows higher expression at both mRNA and protein levels in cardiomyocytes compared to cardiac fibroblasts. Nucleolin is abundant in the nucleolus where it is important for control of cell proliferation and shuttling of pre-RNAs from the nucleus to the cytoplasm (Medina et al., 2010; Tajrishi et al., 2011). We found a strong interaction between nucleolin and mtDNA, 10-fold stronger than nDNA. To our knowledge, this is the first report that extracellular DNA can bind to nucleolin and indicate that nucleolin can transport extracellular DNA taken up by cells.

To identify the subcellular localization of the protein, we investigated pure subcellular fractions and showed by immunoblotting the presence of nucleolin on the membrane of cardiomyocytes, a finding also confirmed by immunocytochemistry. Nucleolin mRNA and protein are expressed in the hearts of rats and mice (Jiang et al., 2013). In that study, Jiang et al. suggested a protective role for nucleolin mediated through **Hsp32 (also known as haem oxygenase1)**. In rats, nucleolin mRNA expression is reduced by about 50% 6 hr after in vivo ischaemia–reperfusion (Jiang et al., 2013). They reported a nucleolin protein band of about 110 kDa, which appears to be cleaved during in vivo ischaemia–reperfusion, as the intensity diminishes simultaneously with the appearance of a 80-kDa band. Species differences and different primary antibodies might account for the relatively high abundance of the ~76-kDa nucleolin band in our study.

Having established that nucleolin was expressed in the cardiomyocyte membrane, we investigated its involvement in internalization of immunogenic DNA. The cell-surface nucleolin blocker midkine (Hovanessian, 2006; Said et al., 2002) reduced the uptake of fluorescent CpG DNA in both cardiomyocytes and cardiac fibroblasts. At the concentration used, midkine did not influence morphology or viability of cardiac cells. It is important to note that midkine is a dual-function cytokine implicated in progression of inflammatory disease, such as experimental autoimmune encephalomyelitis (Wang et al., 2008), but with protective effects in both myocardial infarction (Horiba et al., 2006) and in post-infarction heart failure (Fukui et al., 2008; Takenaka et al., 2009). Midkine has also been suggested to have therapeutic potential in cardiovascular disease in general (Kadomatsu et al., 2014). While the beneficial role of midkine in acute myocardial infarction is fairly well established, its role in heart failure is still debated (Woulfe & Sucharov, 2017). It is tempting to speculate that one of the protective roles of midkine in the acute setting might be via our novel finding of reduced uptake of immunogenic mtDNA in cells. The function of nucleolin in the heart is poorly understood, but it is up-regulated at the mRNA and protein level in human heart failure (Rosello-Lleti et al., 2012). Nucleolin is expressed on the cell surface of many cell types (Fujiki, Watanabe, & Suganuma, 2014), and several lines of evidence underlie the hypothesis that cell-surface nucleolin is important for internalization of DAMPs, including immunogenic DNA. Among others, nucleolin is important for the attachment of HIV-1 to the cell surface of CD4+ T cells (Said et al., 2002) and is required for internalization of human parainfluenza virus type 3 to airway epithelial cells (Bose, Basu, & Banerjee, 2004). Cell-surface nucleolin is the receptor for a 26-mer DNA oligonucleotide (Soundararajan et al., 2009), which is around the same size as the commercial CpGs used in this study. Furthermore, nucleolin mediates the uptake of ~8,000-kDa DNA nanoparticles (Chen et al., 2008), which are slightly larger than CpG DNA (Ribes et al., 2014). Collectively, previous reports create a plausible rationale for the importance of cell-surface nucleolin for internalization of immunogenic DNA.

In conclusion, mtDNA, but not nDNA, trigger an inflammatory response during H/R in cardiomyocytes. H/R and CpG synergistically activate NF-κB via TLR9 in HEK293 cells. Nucleolin is highly expressed in cardiomyocytes, can bind mtDNA, and is mainly expressed on cardiomyocyte membranes. Blocking nucleolin in cardiomyocytes reduces uptake of immunogenic DNA and reduces inflammation. We propose that nucleolin might be a novel target for modulating sterile inflammation after acute myocardial infarction.

ACKNOWLEDGEMENTS

The authors acknowledge the expertise of Gerbrand Koster, PhD, for technical advice and Marte Bliksøen, MD PhD, for critical reading of the manuscript. We also thank Bjørn Dalhus, PhD, and the Regional Core Facility for Structural Biology for help with the nucleolin binding assays. The study was funded by The Norwegian Research Council, Norwegian Health Association, Novo Nordisk Foundation, the South-Eastern Norway Regional Health Authorities (grant 2015095) to the Regional Core Facility for Structural Biology and University of Oslo (Molecular Life Science).

AUTHOR CONTRIBUTIONS

L.H.M. designed the study, and L.H.M. and M.K.T. performed experiments and wrote the first draft of the manuscript. A.B., C.H.M., and Y.L. performed experiments, analysed data, and edited the manuscript. G.V., J.V., and K.O.S. designed the study and analysed data, and J.V. and K.O.S. finalized writing of the manuscript. All co-authors (except G.V.) have approved the manuscript.

CONFLICT OF INTEREST

The authors declare no conflicts of interest.

DECLARATION OF TRANSPARENCY AND SCIENTIFIC RIGOUR

This Declaration acknowledges that this paper adheres to the principles for transparent reporting and scientific rigour of preclinical research as stated in the *BJP* guidelines for Design & Analysis, Immunoblotting and Immunochemistry, and Animal Experimentation, and as recommended by funding agencies, publishers and other organisations engaged with supporting research.

ORCID

Kåre-Olav Stensløkken https://orcid.org/0000-0003-2962-4143

REFERENCES

Alexander, S. P. H., Fabbro, D., Kelly, E., Marrion, N. V., Peters, J. A., Faccenda, E., … Collaborators, C. G. T. P. (2017a). THE CONCISE GUIDE TO PHARMACOLOGY 2017/18: Catalytic receptors. *British Journal of Pharmacology*, *174*, S225–S271. https://doi.org/10.1111/bph.13876

Alexander, S. P. H., Fabbro, D., Kelly, E., Marrion, N. V., Peters, J. A., Faccenda, E., … Collaborators, C. G. T. P. (2017b). THE CONCISE GUIDE TO PHARMACOLOGY 2017/18: Enzymes. *British Journal of Pharmacology*, *174*, S272–S359. https://doi.org/10.1111/bph.13877

Alexander, S. P. H., Kelly, E., Marrion, N. V., Peters, J. A., Faccenda, E., Harding, S. D., … CGTP Collaborators (2017). The concise guide to pharmacology 2017/18: Transporters. *British Journal of Pharmacology*, *174*(Suppl 1), S360–s446. https://doi.org/10.1111/bph.13883

Andrassy, M., Volz, H. C., Igwe, J. C., Funke, B., Eichberger, S. N., Kaya, Z., … Bierhaus, A. (2008). High-mobility group box-1 in ischemia-reperfusion injury of the heart. *Circulation*, *117*, 3216–3226. https://doi.org/10.1161/CIRCULATIONAHA.108.769331

Arslan, F., de Kleijn, D. P., & Pasterkamp, G. (2011). Innate immune signaling in cardiac ischemia. *Nature Reviews. Cardiology*, *8*, 292–300. https://doi.org/10.1038/nrcardio.2011.38

Barth, E., Stammler, G., Speiser, B., & Schaper, J. (1992). Ultrastructural quantitation of mitochondria and myofilaments in cardiac muscle from 10 different animal species including man. *Journal of Molecular and Cellular Cardiology*, *24*, 669–681. https://doi.org/10.1016/0022-2828(92)93381-S

Bliksoen, M., Mariero, L. H., Ohm, I. K., Haugen, F., Yndestad, A., Solheim, S., … Vinge, L. E. (2012). Increased circulating mitochondrial DNA after myocardial infarction. *International Journal of Cardiology*, *158*, 132–134. https://doi.org/10.1016/j.ijcard.2012.04.047

Bliksoen, M., Mariero, L. H., Torp, M. K., Baysa, A., Ytrehus, K., Haugen, F., … Stensløkken, K. O. (2016). Extracellular mtDNA activates NF-κB via toll-like receptor 9 and induces cell death in cardiomyocytes. *Basic Research in Cardiology*, *111*, 42. https://doi.org/10.1007/s00395-016-0553-6

Bose, S., Basu, M., & Banerjee, A. K. (2004). Role of nucleolin in human parainfluenza virus type 3 infection of human lung epithelial cells. *Journal of Virology*, *78*, 8146–8158. https://doi.org/10.1128/JVI.78.15.8146-8158.2004

Chen, X., Kube, D. M., Cooper, M. J., & Davis, P. B. (2008). Cell surface nucleolin serves as receptor for DNA nanoparticles composed of pegylated polylysine and DNA. *Molecular Therapy*, *16*, 333–342. https://doi.org/10.1038/sj.mt.6300365

Collins, L. V., Hajizadeh, S., Holme, E., Jonsson, I. M., & Tarkowski, A. (2004). Endogenously oxidized mitochondrial DNA induces in vivo and in vitro inflammatory responses. *Journal of Leukocyte Biology*, *75*, 995–1000. https://doi.org/10.1189/jlb.0703328

Cong, R., Das, S., & Bouvet, P. (2011). The multiple properties and functions of nucleolin. In J. M. O. Olson (Ed.), *The nucleolus* (pp. 185–212). New York, NY: Springer New York. https://doi.org/10.1007/978-1-4614-0514-6_9

Ding, H. S., Yang, J., Chen, P., Yang, J., Bo, S. Q., Ding, J. W., & Yu, Q. Q. (2013). The HMGB1-TLR4 axis contributes to myocardial ischemia/reperfusion injury via regulation of cardiomyocyte apoptosis. *Gene*, *527*, 389–393. https://doi.org/10.1016/j.gene.2013.05.041

Dutta, D., & Donaldson, J. G. (2012). Search for inhibitors of endocytosis: Intended specificity and unintended consequences. *Cellular Logistics*, *2*, 203–208. https://doi.org/10.4161/cl.23967

Dybdahl, B., Slordahl, S. A., Waage, A., Kierulf, P., Espevik, T., & Sundan, A. (2005). Myocardial ischaemia and the inflammatory response: Release of heat shock protein 70 after myocardial infarction. *Heart*, *91*, 299–304. https://doi.org/10.1136/hrt.2003.028092

Fitzpatrick, S. F., Tambuwala, M. M., Bruning, U., Schaible, B., Scholz, C. C., Byrne, A., … Taylor, C. T. (2011). An intact canonical NF-κB pathway is required for inflammatory gene expression in response to hypoxia. *Journal of Immunology*, *186*, 1091–1096. https://doi.org/10.4049/jimmunol.1002256

Frangogiannis, N. G. (2014). The inflammatory response in myocardial injury, repair, and remodelling. *Nature Reviews. Cardiology*, *11*, 255–265. https://doi.org/10.1038/nrcardio.2014.28

Fujiki, H., Watanabe, T., & Suganuma, M. (2014). Cell-surface nucleolin acts as a central mediator for carcinogenic, anti-carcinogenic, and disease-related ligands. *Journal of Cancer Research and Clinical Oncology*, *140*, 689–699. https://doi.org/10.1007/s00432-014-1587-5

Fukui, S., Kitagawa-Sakakida, S., Kawamata, S., Matsumiya, G., Kawaguchi, N., Matsuura, N., & Sawa, Y. (2008). Therapeutic effect of midkine on cardiac remodeling in infarcted rat hearts. *The Annals of Thoracic Surgery*, *85*, 562–570. https://doi.org/10.1016/j.athoracsur.2007.06.002

Gupta, S., & Knowlton, A. A. (2007). HSP60 trafficking in adult cardiac myocytes: Role of the exosomal pathway. *The American Journal of Physiology*, *292*, H3052–H3056.

Hajizadeh, S., DeGroot, J., TeKoppele, J. M., Tarkowski, A., & Collins, L. V. (2003). Extracellular mitochondrial DNA and oxidatively damaged DNA in synovial fluid of patients with rheumatoid arthritis. *Arthritis Research & Therapy*, *5*, R234–R240. https://doi.org/10.1186/ar787

Harding, S. D., Sharman, J. L., Faccenda, E., Southan, C., Pawson, A. J., Ireland, S., … NC-IUPHAR (2018). The IUPHAR/BPS guide to pharmacology in 2018: Updates and expansion to encompass the new guide to immunopharmacology. *Nucleic Acids Research*, *46*, D1091–d1106. https://doi.org/10.1093/nar/gkx1121

Hemmi, H., Takeuchi, O., Kawai, T., Kaisho, T., Sato, S., Sanjo, H., … Akira, S. (2000). A toll-like receptor recognizes bacterial DNA. *Nature*, *408*, 740–745. https://doi.org/10.1038/35047123

Horiba, M., Kadomatsu, K., Yasui, K., Lee, J. K., Takenaka, H., Sumida, A., … Kodama, I. (2006). Midkine plays a protective role against cardiac ischemia/reperfusion injury through a reduction of apoptotic reaction. *Circulation*, *114*, 1713–1720. https://doi.org/10.1161/CIRCULATIONAHA.106.632273

Hovanessian, A. G. (2006). Midkine, a cytokine that inhibits HIV infection by binding to the cell surface expressed nucleolin. *Cell Research*, *16*, 174–181. https://doi.org/10.1038/sj.cr.7310024

Jiang, B., Liang, P., Wang, K., Lv, C., Sun, L., Tong, Z., … Xiao, X. (2014). Nucleolin involved in myocardial ischaemic preconditioning via post-transcriptional control of HSPA1A expression. *Cardiovascular Research*, *102*, 56–67. https://doi.org/10.1093/cvr/cvu006

Jiang, B., Zhang, B., Liang, P., Chen, G., Zhou, B., Lv, C., … Xiao, X. (2013). Nucleolin protects the heart from ischaemia-reperfusion injury by up-regulating heat shock protein 32. *Cardiovascular Research*, *99*, 92–101. https://doi.org/10.1093/cvr/cvt085

Jiang, B., Zhang, B., Liang, P., Song, J., Deng, H., Tu, Z., … Xiao, X. (2010). Nucleolin/C23 mediates the antiapoptotic effect of heat shock protein 70 during oxidative stress. *The FEBS Journal*, *277*, 642–652. https://doi.org/10.1111/j.1742-4658.2009.07510.x

Kadomatsu, K., Bencsik, P., Gorbe, A., Csonka, C., Sakamoto, K., Kishida, S., & Ferdinandy, P. (2014). Therapeutic potential of midkine in cardiovascular disease. *British Journal of Pharmacology*, *171*, 936–944. https://doi.org/10.1111/bph.12537

Kawai, T., & Akira, S. (2009). The roles of TLRs, RLRs and NLRs in pathogen recognition. *International Immunology*, *21*, 317–337. https://doi.org/10.1093/intimm/dxp017

Kilkenny, C., Browne, W., Cuthill, I. C., Emerson, M., & Altman, D. G. (2010). Animal research: Reporting in vivo experiments: The ARRIVE guidelines. *British Journal of Pharmacology*, *160*, 1577–1579.

Kloner, R. A., Brown, D. A., Csete, M., Dai, W., Downey, J. M., Gottlieb, R. A., … Shi, J. (2017). New and revisited approaches to preserving the reperfused myocardium. *Nature Reviews. Cardiology*, *14*, 679–693. https://doi.org/10.1038/nrcardio.2017.102

la Sala, A., Ferrari, D., Di Virgilio, F., Idzko, M., Norgauer, J., & Girolomoni, G. (2003). Alerting and tuning the immune response by extracellular nucleotides. *Journal of Leukocyte Biology*, *73*, 339–343. https://doi.org/10.1189/jlb.0802418

Medina, F., Fernando, G.-C., Isabel Manzano, A., Manrique, A., & Herranz, R. (2010). Nucleolin, a major conserved multifunctional nucleolar phosphoprotein of proliferating cells. *Journal of Applied Biomedicine*, *8*, 141–150. https://doi.org/10.2478/v10136-009-0017-5

Nakayama, H., & Otsu, K. (2018). Mitochondrial DNA as an inflammatory mediator in cardiovascular diseases. *The Biochemical Journal*, *475*, 839–852. https://doi.org/10.1042/BCJ20170714

Nunez, G. (2011). Intracellular sensors of microbes and danger. *Immunological Reviews*, *243*, 5–8. https://doi.org/10.1111/j.1600-065X.2011.01058.x

O'Connell, T. D., Rodrigo, M. C., & Simpson, P. C. (2007). Isolation and culture of adult mouse cardiac myocytes. *Methods in Molecular Biology*, *357*, 271–296.

Oka, T., Hikoso, S., Yamaguchi, O., Taneike, M., Takeda, T., Tamai, T., … Otsu, K. (2012). Mitochondrial DNA that escapes from autophagy causes inflammation and heart failure. *Nature*, *485*, 251–255. https://doi.org/10.1038/nature10992

Pollack, Y., Kasir, J., Shemer, R., Metzger, S., & Szyf, M. (1984). Methylation pattern of mouse mitochondrial DNA. *Nucleic Acids Research*, *12*, 4811–4824. https://doi.org/10.1093/nar/12.12.4811

Ribes, S., Meister, T., Ott, M., Redlich, S., Janova, H., Hanisch, U. K., … Nau, R. (2014). Intraperitoneal prophylaxis with CpG oligodeoxynucleotides protects neutropenic mice against intracerebral *Escherichia coli* K1 infection. *Journal of Neuroinflammation*, *11*, 14. https://doi.org/10.1186/1742-2094-11-14

Rosello-Lleti, E., Rivera, M., Cortes, R., Azorin, I., Sirera, R., Martinez-Dolz, L., … Portolés, M. (2012). Influence of heart failure on nucleolar organization and protein expression in human hearts. *Biochemical and Biophysical Research Communications*, *418*, 222–228. https://doi.org/10.1016/j.bbrc.2011.12.151

Said, E. A., Krust, B., Nisole, S., Svab, J., Briand, J. P., & Hovanessian, A. G. (2002). The anti-HIV cytokine midkine binds the cell surface-expressed nucleolin as a low affinity receptor. *The Journal of Biological Chemistry*, *277*, 37492–37502. https://doi.org/10.1074/jbc.M201194200

Seong, S. Y., & Matzinger, P. (2004). Hydrophobicity: An ancient damage-associated molecular pattern that initiates innate immune responses. *Nature Reviews. Immunology*, *4*, 469–478. https://doi.org/10.1038/nri1372

Shi, Y., Evans, J. E., & Rock, K. L. (2003). Molecular identification of a danger signal that alerts the immune system to dying cells. *Nature*, *425*, 516–521. https://doi.org/10.1038/nature01991

Soundararajan, S., Wang, L., Sridharan, V., Chen, W., Courtenay-Luck, N., Jones, D., … Fernandes, D. J. (2009). Plasma membrane nucleolin is a receptor for the anticancer aptamer AS1411 in MV4-11 leukemia cells. *Molecular Pharmacology*, *76*, 984–991. https://doi.org/10.1124/mol.109.055947

Tajrishi, M. M., Tuteja, R., & Tuteja, N. (2011). Nucleolin: The most abundant multifunctional phosphoprotein of nucleolus. *Communicative & Integrative Biology*, *4*, 267–275. https://doi.org/10.4161/cib.4.3.14884

Takenaka, H., Horiba, M., Ishiguro, H., Sumida, A., Hojo, M., Usui, A., … Kadomatsu, K. (2009). Midkine prevents ventricular remodeling and improves long-term survival after myocardial infarction. *The American Journal of Physiology*, *296*, H462–H469.

Tian, J., Guo, X., Liu, X. M., Liu, L., Weng, Q. F., Dong, S. J., … Lin, L. (2013). Extracellular HSP60 induces inflammation through activating and up-regulating TLRs in cardiomyocytes. *Cardiovascular Research*, *98*, 391–401. https://doi.org/10.1093/cvr/cvt047

Verthelyi, D., Ishii, K. J., Gursel, M., Takeshita, F., & Klinman, D. M. (2001). Human peripheral blood cells differentially recognize and respond to two distinct CPG motifs. *Journal of Immunology (Baltimore, md: 1950)*, *166*, 2372–2377.

Wang, J., Takeuchi, H., Sonobe, Y., Jin, S., Mizuno, T., Miyakawa, S., … Suzumura, A. (2008). Inhibition of midkine alleviates experimental autoimmune encephalomyelitis through the expansion of regulatory T cell population. *Proceedings of the National Academy of Sciences of the United States of America*, *105*, 3915–3920. https://doi.org/10.1073/pnas.0709592105

Weber, A., Wasiliew, P., & Kracht, M. (2010). Interleukin-1 (IL-1) pathway. *Science Signaling*, *3*, cm1.

Woulfe, K. C., & Sucharov, C. C. (2017). Midkine's role in cardiac pathology. *Journal of Cardiovascular Development and Disease*, *4*, 13.

Zhang, Q., Raoof, M., Chen, Y., Sumi, Y., Sursal, T., Junger, W., … Hauser, C. J. (2010). Circulating mitochondrial DAMPs cause inflammatory responses to injury. *Nature*, *464*, 104–107. https://doi.org/10.1038/nature08780

Zou, N., Ao, L., Cleveland, J. C. Jr., Yang, X., Su, X., Cai, G. Y., … Meng, X. (2008). Critical role of extracellular heat shock cognate protein 70 in the myocardial inflammatory response and cardiac dysfunction after global ischemia-reperfusion. *The American Journal of Physiology*, *294*, H2805–H2813.

SUPPORTING INFORMATION

Additional supporting information may be found online in the Supporting Information section at the end of the article.

How to cite this article: Mariero LH, Torp M-K, Heiestad CM, et al. Inhibiting nucleolin reduce inflammation induced by mitochondrial DNA in cardiomyocytes exposed to hypoxia and reoxygenation. *Br J Pharmacol*. 2019;176:4360–4372. https://doi.org/10.1111/bph.14830